

---

# MULTI-AGENT PATROLLING WITH BATTERY CONSTRAINTS THROUGH DEEP REINFORCEMENT LEARNING

---

**Chenhao Tong**  
The University of Melbourne  
Melbourne, VIC  
chetong@unimelb.edu.au

Aaron Harwood §  
The University of Melbourne  
Melbourne, VIC  
arnhrwd@gmail.com

Maria A. Rodriguez  
The University of Melbourne  
Melbourne, VIC  
marodriguez@unimelb.edu.au

Richard O. Sinnott  
The University of Melbourne  
Melbourne, VIC  
rsinnott@unimelb.edu.au

## ABSTRACT

Autonomous vehicles are suited for continuous area patrolling problems. However, finding an optimal patrolling strategy can be challenging for many reasons. Firstly, patrolling environments are often complex and can include unknown and evolving environmental factors. Secondly, autonomous vehicles can have failures or hardware constraints such as limited battery lives. Importantly, patrolling large areas often requires multiple agents that need to collectively coordinate their actions. In this work, we consider these limitations and propose an approach based on a distributed, model-free deep reinforcement learning based multi-agent patrolling strategy. In this approach, agents make decisions locally based on their own environmental observations and on shared information. In addition, agents are trained to automatically recharge themselves when required to support continuous collective patrolling. A homogeneous multi-agent architecture is proposed, where all patrolling agents have an identical policy. This architecture provides a robust patrolling system that can tolerate agent failures and allow supplementary agents to be added to replace failed agents or to increase the overall patrol performance. This performance is validated through experiments from multiple perspectives, including the overall patrol performance, the efficiency of the battery recharging strategy, the overall robustness of the system, and the agents' ability to adapt to environment dynamics.

**Keywords** Multi-agent system, Multi-agent patrolling, Multi-agent Reinforcement Learning, Deep Reinforcement Learning

## 1 Introduction

*Patrolling* can be defined as travelling regularly through an area so that emerging events of interest, e.g., identifying an intruder, can be identified as early as possible. Autonomous vehicles are highly suited to carry out patrolling tasks. They are designed for continuous and repetitive work, and their usage in hazardous areas leads to reduced safety risks when compared to human labour. The benefits of using autonomous vehicles have been demonstrated in different patrolling use cases such as environment monitoring [31, 18] disaster management [8, 9], and security management [10, 35].

Solutions to the patrolling problem aim to minimize the time between two visits to any location in a given area [16]. However, finding a solution is non-trivial. Chevaleyre [4] has demonstrated that the patrolling problem is highly related to the well-known Travelling Salesman Problem (TSP) and thus is NP-hard. In addition, it is often required to use multiple patrolling agents to patrol a large map, hence, leading to multi-agent coordination problems as well. Existing literature mainly focuses on finding approximate solutions while considering patrolling environments comprising agents that can be accurately modelled. Examples include solutions based on finding short cycles that

---

§Work done while the author was at the University of Melbourne.

cover a given area/map [7, 17], graph partitioning [23, 28, 33], heuristic searches [6], control theory [5], and Bayesian inference [22]. However, in real-world patrolling problems that use of autonomous vehicles as patrolling agents, the complex dynamics of the environment and the limitations of autonomous vehicles further increase the complexity of the problem. In addition, it is unfeasible to model real environments accurately due to their uncertainties. Therefore, a model-free solution to multi-agent patrolling (MAP) problems that takes into consideration real-world factors and constraints is needed.

Multi-Agent Reinforcement Learning (MARL) is a suitable technique for solving many real-world MAP problems. It enables agents to learn, by trial and error, how to make sequential decisions to achieve specific goals in model-free environments. Deep MARL is based on a combination of deep learning and MARL. It has demonstrated its suitability to solve complex real-world multi-agent systems. Recent work in the field has demonstrated that well-trained agents can, for example, outperform professional players in controlling systems such as multi-player real-time strategy games [32]. The success of deep MARL in the automation of real-world multi-agent systems has led to recent interest in applying deep MARL techniques to solving patrolling problems [11, 15].

Despite the recent interest, there remains a lack of studies that provide a comprehensive analysis of real-world MAP requirements and implementations [2]. In fact, the majority of existing MAP solutions based on reinforcement learning [24, 11, 15, 13] assume ideal patrolling environments and agents. As such, they are inadequate for deployment in real-world scenarios.

This work aims to reduce this gap by proposing a solution for MAP problems that factors in different real-world considerations. We follow the existing MARL-based MAP approaches [11, 15] by considering a MAP problem in the environment with uncertainties that cannot be modelled while including two typical real-world limitations of the patrolling agents, which are essential for providing a continuous patrolling performance: battery limitations, and hardware failure problems. The detailed contributions of this paper are as follows:

- We propose a distributed Deep MARL-based MAP approach, where agents maintain a local policy based on their own environmental observations and on information shared by other agents. The approach also takes into consideration the battery constraints of autonomous vehicles, with agents learning to recharge when the battery reaches a critical point.
- A homogeneous multi-agent architecture, where agents have an identical policy. This is used to develop robust patrolling systems that can tolerate agent failures and allow supplementary agents to be added to the system to replace failed agents or to increase the degree of patrolling.
- A multi-objective reward function that evaluates the performance of agent patrols and battery recharging strategies. A modified multi-agent Proximal Policy Optimisation algorithm [26] is proposed to train the agents. The performance of the proposed solution is validated through simulation experiments from three perspectives: patrol performance, the efficiency of the battery recharging strategy, and the overall robustness of the system.

The rest of this paper is organised as follows. Section 2 reviews work on existing MAP solutions. Section 3 illustrates the modelling of the MAP problem as a MARL problem. Section 4 presents the learning algorithm. Section 5 introduces the experiments and discusses the results. Finally, Section 6 concludes the paper and discusses potential areas of future work.

## 2 Related Work

MAP problems can be largely divided into three categories [2, 21]: *adversarial patrolling*, where agents attempt to detect intruders in an area; *area patrolling*, where agents monitor an area for diverse purposes, e.g., information collection, and *perimeter patrolling* which is a special type of area patrolling, where agents monitor the edges of a patrol map. This work focuses on area patrolling.

Machado et al. [16] formalise the definition of the MAP problem as multiple agents continuously traversing a graph  $G(V, E)$  with the aim of minimising the idleness of every vertex. Here the term *idleness* refers to the time between two visits to the same vertex. The authors also compare the performance of several approaches categorised by agents' basic types (cognitive or reactive), agents' observability, communication method, and coordination strategy, and propose two strategies: i) a Conscientious Reactive (CR) strategy, where agents patrol neighbour vertices with the highest degree of idleness, and ii) a Conscientious Cognitive (CC) strategy, where agents follow the shortest path to patrol to the vertex with the highest degree of idleness in the graph. A centralised coordinator is used to ensure no agents target the same vertex. Both methods have been used as baseline strategies for performance comparison in related literature [4, 24, 6, 22, 11]. Chevaleyre [4] demonstrates the MAP problem is closely related to the well-known *Travelling*

*Salesman Problem (TSP)* and thus is NP-hard. The author proposes two graph theory-based strategies: i) a cycle-based strategy where agents follow a cyclic path that connects all vertices, and ii) a graph partition-based strategy where each agent is responsible for patrolling a section of the map. These two approaches have been further explored by many subsequent works [7, 17, 23, 28, 33]. The aforementioned works are largely theoretical, however, and hence cannot be applied to MAP systems deployed in real environments, e.g., they fail to capture factors such as environmental uncertainties due to factors like landscape changes and wind, and vehicle limitations such as sensing limitations and battery constraints.

Several approaches have been proposed to address such challenges. For example, Zhou et al. [37] proposed a Bayesian reinforcement learning-based solution for MAP capable of dealing with uncertain information. Portugal and Rocha [22, 21, 20] proposed a Bayesian rule-based distributed solution that is fault-tolerant and scalable. De Lima et al. [5] proposed a solution based on Supervisory Control Theory that considered safety constraints and modelled the policy with automata [5]. The energy constraints of patrolling agents, although important, have only been studied by a limited number of researchers [29]. Sipahioglu et al. [27] proposed an approach based on the Ulusoy partitioning algorithm that modelled the MAP problem with battery constraints based on a capacitated arc routing problem. Jensen et al. [12] proposed a hot-swap recharging strategy that swapped low-battery agents with fully charged ones [12]. Sugiyama et al. [29] used hierarchical reinforcement learning to train a coordinator that decided how agents should trade off patrolling time and battery recharging time. Basilico and Nicola [2] provided a comprehensive survey of MAP-related literature.

Although multiple real-world factors have been considered by researchers, they typically rely on the construction of models to accurately represent the characteristics of agents and/or the environment. For example, Zhou et al. [37] required the collection of prior knowledge of the environment to construct a Markov Chain in order to train agents. De Lima et al. [5] required a known environment model to build the automata. Sugiyama et al. [29] required prior knowledge of the shortest path from agent locations to battery charging stations. In real-world scenarios, the dynamics of the physical world cannot be accurately modelled due to their stochasticity and complexity, and a priori assumptions made about the environment may not always hold. For instance, the length of the shortest path between two locations is non-deterministic in real-world environments, as the landscape or wind speed and direction can affect the travel time and distance. Even though it is feasible to acquire knowledge of the environment a priori, there is no guarantee that the environmental conditions will remain the same at the time of the actual patrolling. Therefore, an alternative approach is needed.

On the other hand, Multi-agent reinforcement learning (MARL) can solve multi-agent optimization problems without the model of the environment. This allows agents to learn the dynamics of the environment, coordinate strategies, and other sub-tasks without prior knowledge of the system. Santana et al. [24] proposed an RL-based patrolling strategy based on tabular-based Q-Learning to train agents. This was shown to outperform CC and CR strategies [1]. Tabular-based RL algorithms are often suited for small state space problems. For large or infinite state spaces, the alternative is deep MARL, which uses deep neural networks to abstract the information of agent states. Jana et al. [11] trained agents using Deep Q-Learning, with the agents' performance surpassing the CC and CR strategies. Luis et al. [15] carried out real-world lake patrolling experiments to show how deep MARL can be applied to real-world MAP problems. Although existing RL-based patrolling strategies can achieve good performance, the limitations of patrolling agents are not typically considered. To make RL-based solutions more suitable for real-world problems, in this work we consider two typical and significant limitations of patrolling agents: agent battery constraints and their potential failures.

### 3 Preliminaries

#### 3.1 Reinforcement Learning Basics

Reinforcement Learning (RL)<sup>3</sup> is a machine learning approach where an agent interacts with an environment and subsequently learns, by trial and error, how to take a sequence of actions to maximise a long-term cumulative reward. In other words, the agent's goal is to find the optimal policy *policy*, which is a mapping from *states* of the environment to actions the agent should choose that will maximise the long-term cumulative reward. An RL problem is typically modelled as a Markov Decision Process (MDP) given as a set  $\langle S, A, P, R, \gamma \rangle$  where:

- $S$  is the set of all possible states of the environment;
- $A$  is the agent's action space which defines the agents' all available actions;

---

<sup>3</sup>In most of the literature, the term "Reinforcement Learning" usually means Single Agent Reinforcement Learning.

- $P$  is the state transition function of the environment, which tells the probability of the environment transitioning from one state to another given the agent’s action;
- $R$  is the reward function, and
- $\gamma$  is a discount factor where  $\gamma \in [0, 1)$ .

The interaction between the agent and the environment in an RL problem is modelled as follows: in each time step, the agent chooses an action  $a$  from its action space  $A$  according to its policy  $\pi(a | s)$  based on the current environment state  $s$ . The environment will then transition to another state  $s'$  according to the state transition function  $P(s' | s, a)$ , and the agent will receive a reward  $r$  according to the reward function  $R(s, a, s')$ . A sequence of interactions  $(\langle s, a, r \rangle)$  between the agent and the environment, beginning at the initial state of the environment and ending at the terminal state of the environment, is called an episode. The goal of the agent is defined as finding the optimal policy  $\pi^*$  that maximises the expected cumulative reward given as  $\mathcal{R}$  (Eq. 1)

$$\mathcal{R}_t = \sum_{i=0}^{\infty} \gamma^i r_{t+i+1}, \gamma \in [0, 1) \quad (1)$$

where  $\gamma$  is the discount factor that is used to control the influence of future rewards. The larger the value is, the more the agent pursues future rewards. It is also used to converge the cumulative reward to a finite value when dealing with episodes of potentially infinite length.

There are two main types of RL: model-based RL and model-free RL. Model-based RL assumes a known environment state transition function so that the agent can predict the consequence of a given action. Model-free RL does not know the environment model, and the agent learns the consequence of an action only from its past experience when interacting with the environment. In this work, we mainly focus on the model-free RL, as the environment models are generally inaccessible in many real-world problems.

Model-free RL algorithms can be classified into three groups: value-based, policy-based, and actor-critic based. Value-based learning algorithms, such as Q-Learning, use the value iteration method to approach the optimal action-value function  $Q^*$ , and hence obtain the maximum possible expected future return of each available action when the agent is in a given state. An optimal action  $a$  in a given state  $s$  is given as  $\underset{a}{\operatorname{argmax}}(Q^*(s, a))$ . Policy-based algorithms, such as the REINFORCE [34] algorithm, use a policy gradient method to directly update the policy in the direction that results in higher expected returns. Actor-critic algorithms, such as Proximal Policy Optimisation (PPO), combine the previous two types of algorithms to learn a value function (the *critic*), which evaluates the performance of the policy (the *actor*).

One problem that reinforcement learning algorithms face is how to represent the information of the environment state and the agent’s policy. Algorithms such as Q-Learning use a tabular method that stores the mapping between states, actions and the corresponding action values in a table; however, this lacks generalisation and cannot deal with large or infinite state space problems. The alternative approach is Deep Reinforcement Learning, which uses a deep neural network to approximate the action value, state value, and policy function through the use of neural networks.

### 3.2 Multi-agent Reinforcement Learning

Multi-agent Reinforcement Learning (MARL) focuses on decision-making problems involving multiple agents. MARL problems can be classified into three categories based on the relationship between the agents: fully cooperative, fully competitive, and a mixture of the two. In fully cooperative problems, multiple agents cooperate to achieve the same goal. In fully competitive problems, the agents have conflicting interests. In mixed competitive and cooperative problems, agents may have shared interests and conflicting interests. In the latter two types of MARL problems, the concept of the optimal strategy can be replaced by the Nash equilibrium strategy that maximises the worst long-term rewards for different agents. MARL problems can also be classified based on agents’ observability and centralisation, where they can be fully observable or partially observable depending on whether the agents can fully observe the environment state or not, and centralised or decentralised depending on whether the agents can communicate or not. The case with the worst complexity is where agents are decentralised and can only partially observe the environment. This can be modelled by a Decentralised Partially Observable Markov Decision Process (Dec-POMDP) given as a set  $(\mathbb{D}, \mathbf{S}, \mathbb{A}, \mathbf{T}, \mathbf{R}, \gamma, \Omega, \mathbb{O})$  where

- $\mathbb{D}$  is the set of agents in the environment;
- $\mathbf{S}$  is the set of states of the environment;
- $\mathbb{A}$  is the joint actions of all agents, given as  $\mathbb{A} = \times_i \mathbf{A}_i$  where  $\mathbf{A}_i$  is the actions of agent  $i$ ;

- $\mathbf{T}$  is an environment state transition function;
- $\mathbf{R}$  is a reward function;
- $\gamma$  is the discount factor and  $\gamma \in [0, 1]$ ;
- $\Omega$  is the joint observation of all agents, given as  $\Omega = \times_i \Omega_i$  where  $\Omega_i$  is the location observation of agent  $i$ , and
- $\mathbf{O}$  is the observation probability function that specifies the probability distribution of  $\Omega$  given a state action pair.

A special subset of the Dec-POMDP, called Dec-MDP, models situations where the combination of all agent observations is the true state of the environment, that is,  $\Omega = \mathbf{S}$  and  $\mathbf{O}$  becomes deterministic. In addition, if the agents can communicate and form a global observation, Dec-MDP becomes the Multi-Agent MDP (MMDP) – a set  $\langle \mathbf{D}, \mathbf{S}, \mathbf{A}, \mathbf{T}, \mathbf{R}, \gamma \rangle$  where the components are identical to those in the Dec-POMDP set.

### 3.3 Proximal Policy Optimisation Algorithm

The Proximal Policy Optimisation (PPO) algorithm is a state-of-the-art, model-free actor-critic deep RL algorithm. The PPO algorithm is based on the Trust Region Policy Optimization (TRPO) algorithm [25], but it is simpler and has a better sample complexity. Its actor network inputs observations of the environment and outputs a distribution over the action space, with a critic network used to estimate the value of the state. Eq. 2 and Eq. 3 are the loss functions of the actor and critic network of the single agent PPO algorithm [26]. Here:  $T$  is the maximum horizon;  $\theta$  is the neural network parameters;  $r_t$  is the reward at time  $t$ ;  $a_t$  is the agent’s action at time  $t$ ;  $s_t$  is the observed environment state at time  $t$ ;  $\epsilon$  is a clipping constant which limits the value of  $ratio_t(\theta)$  between  $1 - \epsilon$  and  $1 + \epsilon$ ;  $\gamma$  is the discount factor;  $\lambda$  is the discount factor used when calculating  $A_t$ , and  $MSE$  is the *mean square error*.

$$L_t^{CLIP}(\theta) = \mathbb{E}_t[\min(ratio_t(\theta)A_t, \text{clip}(ratio_t(\theta), 1 - \epsilon, 1 + \epsilon)A_t)]$$

$$\text{where } ratio_t(\theta) = \frac{\pi_{\theta_{new}}(a_t | s_t)}{\pi_{\theta_{old}}(a_t | s_t)} \quad (2)$$

$$\text{and } A_t = \delta_t + (\gamma\lambda)\delta_{t+1} + \dots + (\gamma\lambda)^{T-t+1}\delta_{T-1}$$

$$\text{where } \delta_t = r_t + \gamma V_\theta(s_{t+1}) - V_\theta(s_t)$$

$$L_t^{VF}(\theta) = MSE(V_\theta(s_t) - V_t^{targ}(s_t)) \quad (3)$$

The critic network is updated towards the direction where the estimate of the value of the state  $s_t$   $V_\theta(s_t)$  is more accurate to the actual value of the state  $V_t^{targ}(s_t)$ .  $A_t$  is the *Generalized Advantage Estimation*, calculated based on  $V_\theta(s_t)$ . This estimates whether an action leads to a better or worse long-term reward. The loss function of the actor network uses importance sampling, and the idea is to update the policy towards the direction that increases the probability of choosing the action that can lead to a better long-term reward.

To train the agent with the PPO algorithm, a *trajectory* is used based on  $\langle s_t, p(a_t | \theta), r_t, V_\theta(s_t), a_t \rangle$ . This is calculated at each time step of a training episode.  $V_t^{targ}(s_t)$  is approximated based on the cumulative reward at timestamp  $t$ :  $\sum_{t'=t}^T \gamma^{t'-t} r_{t'}$ . The expectation in the loss function of the actor network in Eq. 2 is approximated based on the sample mean as shown in Eq. 4, where  $K$  is the sample set.

$$\overline{L_t^{CLIP}(\theta)} = \frac{\sum_{t \in K} \min(ratio_t(\theta)A_t, \text{clip}(ratio_t(\theta), 1 - \epsilon, 1 + \epsilon)A_t)}{|K|} \quad (4)$$

## 4 Problem Modelling

Following the work of Machado et al. [16], we consider the MAP problem as a set of agents  $A$  continuously traversing a graph  $G(V, E)$  with the goal of minimising the idleness of every vertex. For modelling purposes, we define the following:

- $Idle(v_t)$  – the idleness of vertex  $v$  at time  $t$ ;

- $Idle(G_t)$  – the idleness of graph  $G(V, E)$  at time  $t$ , which is the average of the idleness of all vertices in the graph  $G(V, E)$ ;
- $AVG^h(G)$  – the average of  $Idle(G)$  over  $h$  steps of a patrolling scenario, and
- $MAX^h(G)$  – the maximum  $Idle(v_t)$  that occurs during  $h$  steps of a given patrolling scenario.

The patrolling problem can be modelled as an optimisation problem, with two commonly used optimisation criteria [16, 4, 24, 11, 22]: i) minimising  $AVG^h(G)$ , and ii) minimising  $MAX^h(G)$ .  $AVG^h(G)$  and  $MAX^h(G)$  are also commonly used as criteria for measuring the patrolling performance of a policy. For clarity, when referring to the performance evaluation result of a specific policy  $\pi$ ,  $AVG^h(G)$  and  $MAX^h(G)$  are written as  $AVG_\pi^h(G)$  and  $MAX_\pi^h(G)$ .

Many existing works only consider one of the two optimisation criteria [4, 24, 22, 11, 15]. However, it is shown by Santana et al. [24] that given two policies  $\pi_A$  and  $\pi_B$ :

$$\begin{aligned} MAX_{\pi_A}^h(G) > MAX_{\pi_B}^h(G) &\not\Rightarrow AVG_{\pi_A}^h(G) > AVG_{\pi_B}^h(G) \\ \text{and} & \\ AVG_{\pi_A}^h(G) > AVG_{\pi_B}^h(G) &\not\Rightarrow MAX_{\pi_A}^h(G) > MAX_{\pi_B}^h(G) \end{aligned} \quad (5)$$

In other words, only considering one criterion may lead to the other criterion not being optimised. Therefore, both optimisation goals are taken into account in this work.

In this work, since autonomous vehicles are used as patrolling agents, we take into account the vehicle's (agent) battery limitations and potential failures. With regard to battery limitations, we assume that agents must recharge their batteries before they run out to enable continuous patrolling. However, the time used to recharge a modern autonomous vehicle, e.g., a UAV, can be up to four times longer than the actual flight time [30]. Therefore, it is impractical to wait until a vehicle is fully charged before deploying it to continue a given patrol. Instead, in this work, we assume a hot-swap battery recharging scheme [12], i.e., when a vehicle goes to the battery charging station for recharge, a fully charged vehicle will be deployed to replace it. In addition, we do not assume that the hot-swap procedure can be done instantly since, in real-world scenarios, hardware checking and other maintenance works might need to be carried out before an autonomous vehicle can be safely deployed.

The battery constraint makes the second optimisation criteria, minimising  $MAX^h(G)$ , inapplicable, since the highest  $Idle(v_t)$  is likely to occur during an agent's recharging time as fewer agents are patrolling the map, hence this does not reflect agents' actual patrolling performance. Instead, we use the average of the highest  $Idle(v_t)$  measured at each time step over  $h$  steps of a given patrolling scenario. This also serves the purpose of measuring the worst patrolling performance of the agent. For clarity, we abbreviate this as  $\overline{MAX}^h(G)$ . With regard to failure problems, when a patrolling vehicle fails, a supplementary vehicle can be deployed from the battery charging station to replace the failed agents. However, online agents need to ensure the patrolling task does not fail, e.g., failing to patrol some areas for too long, before the supplementary agent is deployed.

In this section, we introduce how we model the patrolling environment and the agents, and how they interact with each other in the patrolling scenario. We begin by introducing the assumptions made about the system:

- the hot-swap procedure takes constant time to execute and equals the time to deploy a supplementary agent;
- the patrolling graph does not change during patrolling, and the patrolling agents know the graph in advance;
- all agents take actions simultaneously at each time step;
- we assume the communication between agents has no cost or delay so that all agents can share their local information with each other to form a global observation and choose actions accordingly. Minimal data transfer between agents is required to make this assumption valid in real-world scenarios;
- when an agent fails, it can be replaced by a supplementary agent. The time to deploy a supplementary agent equals the time to execute the hot-swap procedure. It is also assumed that there always have supplementary agents to replace the failure agents;
- we consider the patrolling graph on a large scale so that each vertex is large enough for multiple agents to visit at the same time;
- the battery charging station has enough charging slots to charge all agents simultaneously and has enough supplementary agents to replace potentially all charging agents.

## 4.1 Environment and Agent Modelling

The graph that is patrolled by autonomous vehicles is based on a geometric graph, which can be discretised into a grid and represented as a matrix. Fig. 1a shows an example of a grid map, where grey blocks are vertices (i.e., locations that agents can visit), white blocks are obstacles (i.e., locations that agents cannot occupy), the black block is the battery charging station, and the circle represents a given agent. Fig. 1b is the matrix representation of the grid map in Fig. 1a, where 0 represents the vertices,  $-1$  represents obstacles, and 1 represents battery charging stations. The location of the agent is represented by the matrix index of the vertex occupied by the agent, which simulates the GPS coordinates of the agent in real-world scenarios. For example, in Fig. 1a, if the top-left block has index  $(0, 0)$ , then the bottom-right block has index  $(5, 5)$ , and the location of the agent is  $(1, 2)$ . In this work, it is assumed that the agent always knows its current location. In addition, as agents are patrolling grid maps, it is assumed that the action space of the agent is one of  $\langle Up, Down, Left, Right \rangle$ .

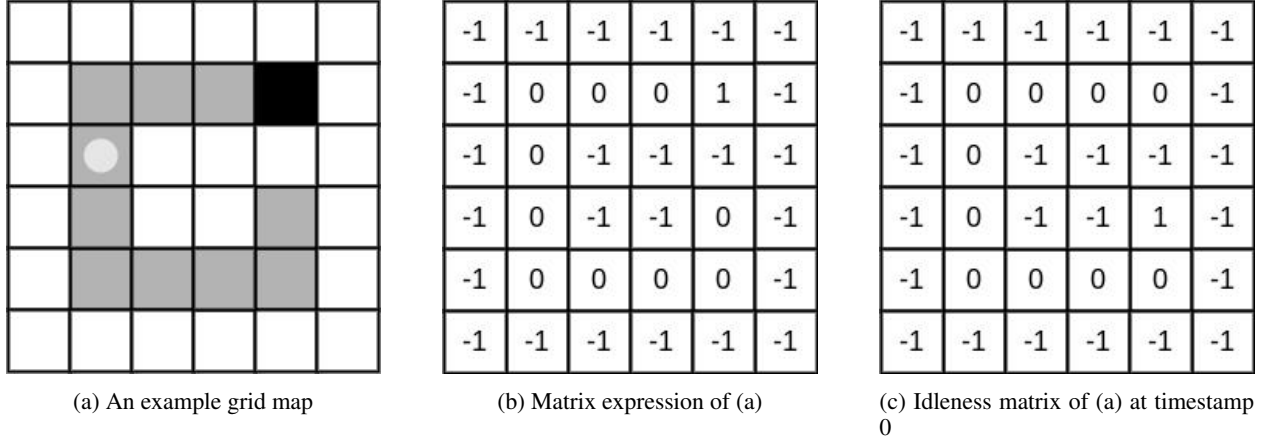


Figure 1: An example grid map (a), and its corresponding matrix expression (b) and its idleness matrix at timestamp 0.

Similarly, the idleness of the grid map can also be represented by a matrix. It is assumed that the idleness of vertices is 0 at the beginning of a patrolling scenario, and that this will increment at a constant rate at each time step. If a vertex is visited by an agent, the idleness of that vertex will be reset to 0. The idleness of obstacles remains constant at  $-1$ , and the idleness of the battery charging station is always 0. Fig. 1c shows the idleness matrix for the grid map in Fig. 1a at time 0. As we assume that agents can communicate, they can share their current locations with each other to form a real-time global observation of the idleness matrix of the graph.

An agent's remaining battery information is represented by the percentage of the remaining battery capacity. Agents share their remaining battery information with each other. When an agent goes to the battery charging station for a recharge, other agents know the progress of the hot-swapping procedure, given as the percentage of completion.

Overall, the observable information of the environment at time  $t$  is given as a set  $\langle G(V, E), Idle(G_t), B_t, Loc_t, RCP_t \rangle$ , where  $Idle(G_t)$  is the idleness matrix of the graph  $G(V, E)$  at time  $t$ ,  $B_t$  is a given agent's remaining battery level at time  $t$ ,  $Loc_t$  is an agent's location information at time  $t$ , and  $RCP_t$  is the charging agent's hot-swap recharging progress at time  $t$ .

## 4.2 Environment State Transitions

In a given patrolling scenario, agents interact with the environment in the following way:

1. At time step 0, i.e., at the beginning of a patrolling scenario, all agents are randomly placed on vertices in the graph, and their batteries will be fully charged.
2. At the start of each time step, all vertices' idleness will increase by a fixed amount, and all agents' remaining battery life will decrease by a fixed amount.
3. At each time step, each agent will first share their local information with other agents to form a global observation. Based on the global observation, each agent will choose an action, and all agents will act simultaneously and move to the corresponding vertex in the direction of the action.
4. If the agent lands on the battery charging station, the hot-swap procedure will start immediately, and a supplementary agent will be deployed, which takes constant time to complete. The recharging agent and the

supplementary agent before deployment are considered offline, therefore, they cannot take any actions or make any observations.

5. At the end of each time step, the idleness of the vertices occupied by agents will be set to 0.

The following two scenarios are considered catastrophic failures, resulting in the termination of a patrolling scenario: i) if any of the agents runs out of battery or ii) if the idleness of a vertex reaches a predefined threshold, i.e., the vertex has not been visited by any agent for a defined period of time.

## 5 Methods

To solve the MAP problem as a reinforcement learning problem, an MDP is required to model the problem. In this work, agents can communicate and share their local observations, and the number of agents will vary due to failed agents or the introduction of supplementary ones. Therefore, a distribution of Multi-agent Markov Decision Processes (MMDP)  $\tau_t \sim p(\tau)$  is proposed to model the MAP problem, where  $\tau_t = \langle \mathbb{D}_t, \mathbf{S}, \mathbb{A}_t, \mathbf{T}, \mathbf{R}, \gamma \rangle$  is an MMDP where:  $\mathbb{D}_t$  is the set of agents at time step  $t$ ; and  $\mathbb{A}_t$  is the agents' corresponding joint action space at time step  $t$ . The other components are identical to those in Dec-POMDP. In this section, we will detailedly introduce the reward function, the patrolling system architecture, and the learning algorithm proposed to solve the problem.

### 5.1 The Reward Function

The reward function reflects the performance of the agent's policy on solving a given task. In this work, the reward function evaluates agents from two perspectives: i) the performance of the agents' patrolling strategy, and ii) the performance of the agents' battery charging strategy. Therefore, the MAP problem we are considering can be treated as a multi-objective reinforcement learning problem, with two reward functions,  $R_i$  and  $R_b$ , evaluating the agents from each of the two perspectives. The linear scalarization method is used to combine the two reward functions into a single reward function with a weighted sum function, as shown in Eq. 6, where  $w_i$  and  $w_b$  are the respective weight coefficients.

$$r = w_i \cdot R_i + w_b \cdot R_b \quad (6)$$

**Patrolling performance ( $R_i$ )** With respect to the agents' patrolling goal, two optimisation criteria are considered:  $AVG^h(G)$  and  $\overline{MAX^h(G)}$ . Similarly, the linear scalarization method is used; we combine the two criteria with the summation function since we consider both criteria to be equally important. The optimisation goal is then to minimise  $AVG^h(G) + \overline{MAX^h(G)}$ , which is equivalent to maximising  $-AVG^h(G) - \overline{MAX^h(G)}$ . Therefore, the  $R_i$  is defined as:

$$R_i = -AVG^h(G) - \overline{MAX^h(G)} \quad (7)$$

and the corresponding cumulative reward function with finite horizon  $h$  is shown in Eq. 8. The reinforcement learning algorithm will find a strategy that maximises Eq. 8, hence, solving the defined problem.

$$\mathcal{R}_i = \sum_{t=0}^h \gamma^t \cdot (-AVG^h(G) - \overline{MAX^h(G)}) \quad (8)$$

For convenience, the idleness of vertices will be normalised between 0 and 1 by dividing the idleness of a vertex by the idleness threshold.  $R_i$  is scaled to a positive reward with value between 0 and 1, as shown in Eq. 9

$$R_i = \frac{2 - AVG^h(G) - \overline{MAX^h(G)}}{2} \quad (9)$$

**Battery usage ( $R_b$ )** With respect to the performance of the agents' battery charging strategy, as we consider a hot-swap battery recharging scheme, agents are encouraged to almost fully expend their battery before recharging. This reduces the number of visits to the charging station and, thus, the number of backup agents that are required. The recharging strategy of an agent is evaluated based on two aspects: i) the ability of an agent to recharge its battery before it runs out as measured by  $R_{b1}$ , and ii) the ability of an agent to avoid unnecessary charging as measured by  $R_{b2}$ . Again, the linear scalarization method is used, and  $R_b$  is defined as:

$$R_b = R_{b1} + R_{b2} \quad (10)$$

An agent  $k$  failing to recharge its battery will be penalised by a constant value, as shown in Eq. 11.

$$R_{b1}(k) = \begin{cases} -c_b & \text{if agent } k \text{ runs out of battery} \\ 0 & \text{Otherwise} \end{cases} \quad (11)$$

Agents should use *most* of their battery before recharging. Our approach encourages agents to arrive at charging stations with *approximately* 10% of the battery remaining. This contingency is allowed with the aim of avoiding scenarios where agents run out of battery while patrolling. Eq. 12 estimates  $R_{b2}$  for agent  $k$ :

$$R_{b2}(k) = \begin{cases} -\log_{10}^2(10 \cdot b_k + 0.01) & * \\ 0 & \text{Otherwise} \end{cases} \quad (12)$$

\* -if agent  $k$  lands on the battery charging station

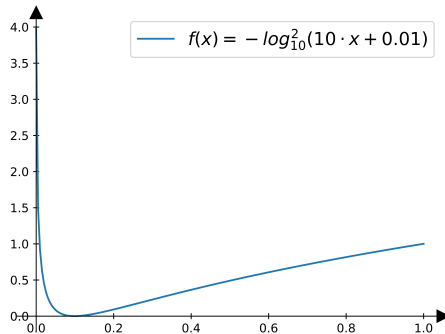


Figure 2: Function plot of  $f(x) = -\log_{10}^2(10 \cdot x + 0.01), x \in [0, 1]$

where  $b_k$  is agent  $k$ 's remaining battery level when arriving at the battery charging station. Fig. 2 plots  $f(x) = -\log_{10}^2(10 \cdot x + 0.01), x \in [0, 1]$ . From the graph, we can see that when an agent recharges with 9.9% of remaining battery, the agent's recharging strategy is considered optimal and, therefore, will not receive a penalty. Otherwise, a penalty will be assigned to the agent.

It is worth noting that all agents will receive the same reward  $R_i$ , but  $R_b$  is specific to each agent. Therefore, the reward function  $R$  used in this work is heterogeneous. For convenience, when referencing agent  $i$ 's reward at time step  $t$ , we use the convention  $R_t(i)$ .

## 5.2 System Architecture

The design of the architecture of the patrolling system should take robustness into account, that is, the system should tolerate losing some agents and should allow the introduction of supplementary agents. A heterogeneous multi-agent system (MAS) architecture is commonly used in previous RL-based MAP approaches [24, 11], where agents have distinct policies and are able to learn individually. In a heterogeneous MAS with  $n$  agents, the number of possible combinations of agents that are online (i.e., patrolling) at any given point in time is  $2^n - 1$ , without considering the case in which all agents are offline. In order to train a robust strategy that tolerates changes to the number of patrolling agents, the agents would have to learn to cooperate with each other in  $2^n - 1$  distinct cases, requiring a vast amount of training samples to cover all patrolling situations. In addition, scaling up becomes challenging under such an architecture, as determining the policy that newly added agents will follow is not straightforward. One approach is to let additional agents execute random policies from existing agents, but this may lead to inconsistent performance. Therefore, in this work, we consider a homogeneous MAS architecture, where agents have identical policies. With  $n$  agents, the number of possible combinations of online agents at any time is  $n - 1$ , requiring fewer samples to train a robust (patrolling) policy. In addition, since agents are identical, the experience (learning) can be shared between them to improve sample efficiency. Moreover, agents are potentially trained to have a strategy that can cooperate with a varying number of agents. Therefore, when scaling up the system, it is expected that the additional agents can cooperate well with the existing agents in the system.

In addition, a distributed patrolling strategy without a central coordinator is required when designing a robust patrolling system. Otherwise, when agents lose communication with the coordinator, the system will fail catastrophically. Therefore, in this work, the agent’s policy is designed only depending on the agent’s local observation and shared information from other agents, and the agent will decide its action locally. When a network partition occurs, the agents disconnected from the communication network can be considered offline, while the rest of the agents have been trained on how to handle failed agent scenarios, therefore, catastrophic failure of the patrolling system is less likely to occur.

### 5.3 The Learning Algorithm

In this work, deep MARL is used, where agents use deep neural networks to approximate the information of the states or policies, which allows them to be generalised to diverse patrolling situations. However, a varying number of agents results in an observation space of varying size, which cannot be easily handled by many deep neural network architectures, such as Convolutional Neural Networks (CNNs) and Artificial Neural Network (ANNs). The observable information from the environment and other agents is a set  $\langle G(V, E), Idle(G_t), B_t, Loc_t, ACT_i, RCP_t \rangle$ . The size of the graph  $G$ , the idleness matrix  $Idle(G_t)$ , and the invalid action masking set  $ACT_i$  are constant, while the size of the agents’ locations information  $Loc_t$ , batteries information  $B_t$ , and progress of the hot-swap procedures  $RCP_t$  vary with respect to the number of active agents. Therefore,  $\langle Loc_t, B_t, RCP_t \rangle$  need to be transformed into fixed-size expressions.

For  $Loc_t$ , the agent will set the idleness of the vertices occupied by other agents to 0 in the idleness matrix after establishing the agents’ locations. Since only the vertices occupied by agents will have an idleness value of 0, all agents’ location information can be derived from the idleness matrix. However, an agent still needs to know its current coordinate  $Loc_{it}$  to be able to differentiate which vertex with idleness 0 is occupied by itself.

For  $B_t$  and  $RCP_t$ , during the training time, we assumed a maximum number of agents, resulting in a bounded size of  $B_t$  and  $RCP_t$ , and therefore,  $B_t$  and  $RCP_t$  can be included in the agents’ observation. However, during the run time, the maximum number of agents is unknown, resulting in an unbound size of  $B_t$  and  $RCP_t$ , and therefore, we can exclude  $B_t$  and  $RCP_t$  from the agents’ observation because an agent can still recharge near optimally with its local battery information. However, this results in agents’ observations being inconsistent during the training time and the run time. To solve the problem, the centralised training and decentralised execution actor-critic reinforcement learning (CTDE AC RL) framework [14] is used, where the actor network, i.e., the agent’s policy, runs locally in each agent based on its local and shared observations. The critic network, on the other hand, runs centrally based on global observations and evaluates the values of states *during training*. Therefore,  $B_t$  and  $RCP_t$  are given to the agent’s critic network, while an agent  $i$ ’s actor network is given the  $B_{it}$ . In addition, all agents’ location information  $Loc_t$ , is also given to the critic network.

In addition, to train the agents to avoid hitting obstacles, the invalid action masking method is used [32], which inputs the validity of actions as an observation to the agent, and renormalises the agents’ probability distribution of the action space so that only valid actions can be chosen. In this paper, a set with four elements is used to represent the validity of each of the four actions, with entries in the set being 0 if the action is invalid or 1 otherwise. For example, in the scenario depicted in Figure 1a, the agent can only move *Up* or *Down*, resulting in the following action masking set:  $\langle 1, 1, 0, 0 \rangle$ , and the invalid action masking set will be given to the actor network as an observation since it is irrelevant when evaluating the value of the state; and if assume the agent’s probability distribution over the action space is  $\langle 0.4, 0.1, 0.3, 0.2 \rangle$ , since actions ”Left” and ”Right” are invalid, the probability distribution will be renormalised to  $\langle 0.8, 0.2, 0, 0 \rangle$ . In real-world scenarios, the invalid action masking set can be acquired by obstacle detection hardware, e.g. radar.

In summary, the observation input to the critic network at time step  $t$  ( $O_t^c$ ) is a set  $\langle G(V, E), Idle(G_t), B_t, Loc_t, RCP_t \rangle$ , and the observation input to the agent  $i$ ’s actor network at timestep  $t$  ( $O_{it}^a$ ) is  $\langle G(V, E), Idle(G_t), B_{it}, Loc_{it}, ACT_{it} \rangle$ .

In this work, we modify the Multi-agent Proximal Policy Optimization (MAPPO) algorithm [26, 36] to train our strategy. The details will be introduced in the next section.

#### 5.3.1 Multi-agent Proximal Policy Optimization Algorithm

MAPPO is a deep MARL algorithm following the CTDE AC framework, which uses a critic network  $V_{\theta_1}(s)$  with parameter set  $\theta_1$  to evaluate the value of the state, and uses an actor network  $\pi_{\theta_2}(s)$  with parameter set  $\theta_2$  to approximate the agent’s policy. The detailed architectures of the actor and critic networks used in this work are illustrated in Figure 3a and 3b.

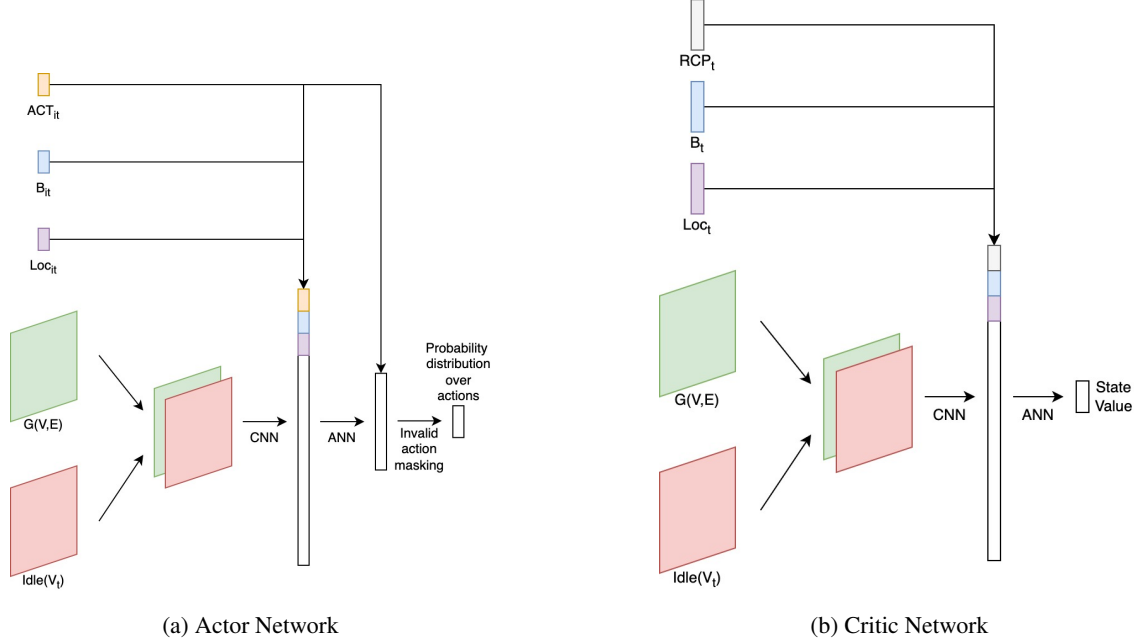


Figure 3: Architecture of the Actor Network 3a and the Critic Network 3b in the MAPPO. The arrow represents the direction of the data flow.

First, the grid map and the idleness matrix are concatenated and processed by a CNN. The output of the CNN is then flattened as a one-dimensional array. For clarity, the flattened CNN output of the critic network is named  $O_{CNN}^c$ , and the flattened CNN output of the actor network is named  $O_{CNN}^a$ . For the critic network, observations  $Loc_t$ ,  $B_t$  and  $RCP_t$  are included as part of  $O_{CNN}^c$ , which is the input to an ANN, producing as output an estimate of the value of the state at time step  $t$  ( $V_{\theta_1}(s_t)$ ). For the actor network,  $Loc_{it}$ ,  $B_{it}$  and  $ACT_{it}$  are included as part of  $O_{CNN}^a$ , which is the input to an ANN, producing as out the probability distribution over the action space ( $p_{\theta_2}(a | s_t)$ ); then, renormalised according to the invalid masking set to avoid agents choosing invalid actions.

In our multi-agent patrolling scenario, the heterogeneous reward function results in different agents calculating different values of  $V_t^{target}(s_t)$ , which introduces instabilities. Therefore, a scalarization function is used to map each agent’s  $V_t^{target}(s_t)$  to a single value. Since all agents are using the same policy  $\pi$ , the performance of the policy  $\pi$  can be approximated by the average performance of all agents, represented by the average of the cumulative rewards of all agents. Therefore, the average function is used as the scalarization function when calculating  $V_t^{target}(s_t)$ . The expression of  $V_t^{target}(s_t)$  is shown in Eq. 13:

$$V_t^{target}(s_t) = \frac{\sum_{d \in D} \sum_{t'=t}^T \gamma^{t'-t} r_{dt'}}{|D|} \quad (13)$$

where  $D$  is the set of agents,  $r_{dt'}$  is agent  $d$ ’s reward at time  $t'$ . The actor loss function remains the same.

### 5.3.2 Trajectory Collection

As it is introduced in Section. 3, training agents with PPO requires a trajectory containing  $\langle s_t, p(a_t | \theta), r_t, V_{\theta}(s_t), a_t \rangle$  to be collected in each time step of a training episode. In this work, as the homogeneous MAS architecture is used, agents will collect their trajectories locally during the training episode, and the trajectories will be combined together after the training episode is terminated. A failed or recharging agent is considered offline and will be replaced by

a supplementary agent, and the supplementary agent will continue the trajectory collection. However, deploying a supplementary agent takes time, which means that the trajectory is not collected when preparing the supplementary agent for deployment.

This will lead to the problem that, even if agents are receiving identical rewards, they will still calculate different values of  $V_t^{target}(s_t)$  for the same state  $s_t$ , which should be identical, and therefore, introduces instability. For example, assume that two agents  $a$  and  $b$  run an episode for 10 steps and are receiving identical rewards with the discount factor  $\gamma = 1$ . Agent  $a$  recharges itself at timestamp 1, and agent  $b$  recharges itself at timestamp 3, and deploying a supplementary agent takes 6 timesteps. The  $V_t^{target}(s_0)$  calculated by agent  $a$  is  $\mathcal{R}_a(s_0) = r_0 + r_7 + r_8 + r_9$ , and the  $V_t^{target}(s_0)$  calculated by agent  $b$  is  $\mathcal{R}_b(s_0) = r_0 + r_1 + r_2 + r_9$ . And  $\mathcal{R}_a(s_0) \neq \mathcal{R}_b(s_0)$ .

However, using a homogeneous MAS architecture enables trajectory data to be shared between agents. By doing this, missing data not collected during the deployment of a supplementary agent can be reconstructed based on the trajectories of other running agents. In the example above, the cumulative reward of  $s_0$  calculated by both agents  $a$  and  $b$  now becomes  $r_0 + r_1 + r_2 + r_7 + r_8 + r_9$ . During time 3 to time 6, no agents are patrolling, so no data can be shared between the agents. By using this method, all agents will calculate the same  $V_t^{target}(s_t)$ , which reduces the instability. In addition, the trajectories from different agents can be concatenated together to form a larger trajectory to train the agents, therefore, improving the sample efficiency.

The pseudocode of the learning algorithm is shown in Algorithm 1.

---

**Algorithm 1** Homogeneous Multi-agent Proximal Policy Optimisation Algorithm

---

```

1:  $i \leftarrow 0$ 
2: Create an agent ( $agent_0$ )
3: Initialise  $agent_0$ 's Actor and Critic Network with random parameters
4: Clone the  $agent_0$  into  $N$  agents
5: while  $i \leq episodes$  do
6:   Reset the environment
7:    $s \leftarrow$  starting state  $s_0$ 
8:    $step \leftarrow 0$ 
9:   while  $step \leq horizon$  or episode is not terminated do
10:     $joint\_action \leftarrow []$ 
11:    Each agent  $i$  makes an observation and shares its location with other agents to form  $O_t^c$  and  $O_{it}^a$ 
12:     $V_{\theta_1}(s_t) \leftarrow critic\_network(O_t^c)$ 
13:    for each online agent  $a$  do
14:       $joint\_action.append(a.actor(O_{it}^a))$ 
15:    end for
16:    update environment
17:     $s \leftarrow new\_state$ 
18:    each agent store  $\langle O_t^c, O_{it}^a, p(a_{it} | \theta), r_t(i), V_{\theta_1}(s_t), a_{it} \rangle$ 
19:    if any agent's battery expires or idleness expires then
20:      terminate episode
21:    else
22:       $step \leftarrow step + 1$ 
23:    end if
24:    all agents except  $agent_0$  copy memory to  $agent_0$ 
25:     $agent_0$  update actor and critic network
26:    for each agent  $a$  except  $agent_0$  do
27:       $a.actor \leftarrow agent_0.actor$ 
28:       $a.critic \leftarrow agent_0.critic$ 
29:    end for
30:  end while
31: end while

```

---

## 6 Performance evaluation

In this work, the training and evaluation experiments are performed based on two patrolling maps: Map A shown in Fig. 4b, with 75 vertices (including battery charging stations) and 91 edges; and Map B shown in 4a), with 75 vertices

(including battery charging stations) and 121 edges. Given that Map B has more edges than Map A, Map B is more complex and harder for the agents to learn how to optimally patrol. It is assumed that the threshold of the maximum idleness is 750, the maximum capacity of the agent’s battery allows the agent to move 750 steps, and the hot-swap procedure takes 50 steps to complete.

We evaluate the performance of the deep MARL-based strategy from the following perspectives:

- **Patrolling performance** – evaluated based on the *idleness failure rate* (when the idleness of any vertex exceeds the given threshold) and on the performance criteria  $AVG^h(G)$  and  $MAX^h(G)$  (as defined in Section 4). The lower the idleness failure rate and the lower the values of the performance criteria, the better the strategy’s patrolling performance;
- **Battery recharging performance** – evaluated based on the *battery failure rate* (when an agent runs out of battery) and on the remaining battery level when agents recharge. The lower the battery failure rate and the closer the agent’s remaining battery is to 10% when recharging, the better the strategy’s battery recharging performance;
- **Robustness** – evaluated based on the patrolling and battery recharging performance of the strategy in situations when agents fail or when supplementary agents are introduced to the system. A robust patrolling strategy should not suffer significant degradation in performance when agent failures occur and when supplementary agents are introduced. It is expected that new agents will automatically cooperate with existing ones to increase the performance of the patrolling system. Fig 1a

In addition, we evaluate the strategies’ ability to adapt to unexpected agent behaviour caused by dynamics in the environment, such as wind or landscape. Specifically, we consider situations in which the agents’ ability to move in a given direction is affected by environmental factors. The smaller the effect on the strategy’s performance, the better the adaptability.

As baseline strategies for performance comparison, we consider CC and CR. For fairness, the agents with CC and CR strategies are allowed to communicate and form a global observation of the idleness matrix. The original CC and CR strategies do not include a battery charging strategy, therefore, we extend their definition to enable agents to follow the shortest path to the nearest battery charging station when their battery level reaches a critical point. It is worth noting that in the case of CR, when multiple agents visit the same vertex at the same time (allowed based on our problem formulation), the following actions they take will be identical, causing them to follow the same patrolling path henceforth. This leads to a degraded patrolling performance. To address this issue, agents controlled by a CR strategy move randomly to a nearby vertex with a 5% probability at every step, except when they go to recharge. In addition, when testing the performance of the agents in a dynamic environment, the shortest path algorithm may no longer work as the agents may not be able to follow the shortest path; hence the CC and CR strategies will not be used for performance comparison in this case.

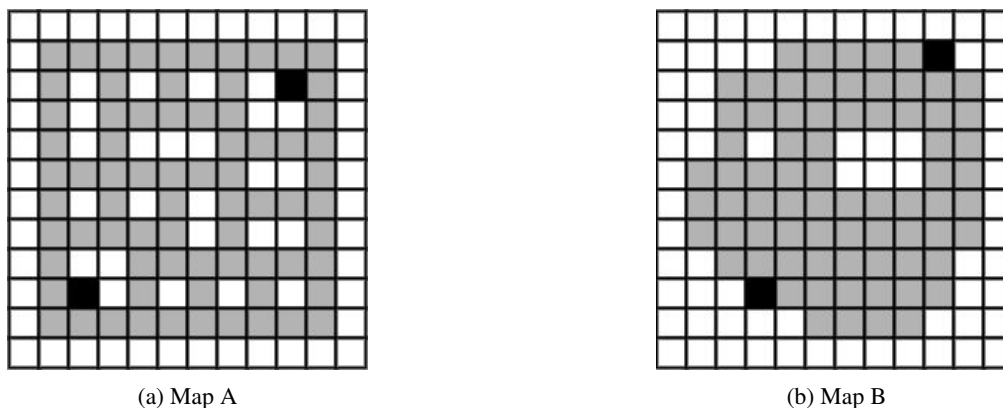


Figure 4: Two patrolling maps. Map A has 75 vertices and 91 edges, Map B has 75 vertices and 123 edges.

## 6.1 Training results

To analyse the performance of the deep MARL-based approach, we train and test 3 strategies for each map using a different number of agents - 2, 3 and 4. We do not consider a single-agent scenario since it is not a multi-agent system problem. Each strategy is trained using 60,000 episodes, with each training episode having 2,000 steps. With respect

Layer	Parameter	Activation Function
Conv	ic=2, oc=4, ks=(3,3), s=1, p=0	Tanh
Conv	ic=4, oc=6, ks=(3,3), s=1, p=0	Tanh
Dense	391 × 260	Tanh
Dense	260 × 173	Tanh
Dense	173 × 115	Tanh
Dense	115 × 4	None

Table 1: Neural network architecture of the agent’s actor network. ”Conv” – convolutional layer, ”Dense” – dense layer, ”ic” – ”input channel”. ”oc” – ”output channel”. ”ks” – ”kernel size”. ”s” – ”stride”. ”p” – ”padding”.

Layer	Parameter	Activation Function
Conv	ic=2, oc=4, ks=(3,3), s=1, p=0	Tanh
Conv	ic=4, oc=6, ks=(3,3), s=1, p=0	Tanh
Dense	392 × 260 (2 agents), 396 × 260 (3 agents), 400 × 260 (4 agents)	Tanh
Dense	260 × 173	Tanh
Dense	173 × 115	Tanh
Dense	115 × 1	None

Table 2: Neural network architecture of the agent’s critic network.

to training strategies that are robust, the scenarios in which agents need to recharge repeatedly are similar to agent failure scenarios – the number of agents varies in both cases. Therefore, it is assumed that no additional training is required to train robust strategies. The details of the architecture of the agent’s actor and critic networks are shown in the in Table 1 and 2, and the training hyperparameters of the MAPPO algorithm are shown in Table 3. The coefficients in the reward function are shown in Table 4.

For simplicity, we use the following convention to name different versions of the deep MARL-based strategy:  $TnA/B$ , where  $n$  is the number of agents with which the strategy was trained and  $A/B$  represents whether agents are trained on Map A or Map B. For example,  $T3A$  represents a strategy trained with 3 agents on Map A. In cases in which the Map is not relevant,  $TnA/B$  is abbreviated as  $Tn$ .

Fig. 5 demonstrates the training results of different strategies on the two maps. Fig. 5a to Fig. 5f show the cumulative reward that the agents gain, which is normalised between 0 to 1000. Fig. 5g to Fig. 5l show the average battery level when the agents recharge in each episode of the training process. If agents have not recharged in an episode, the average battery remaining in that episode will be set to 1. In the graph, the points depict the cumulative reward (the average battery remaining when agents recharge), and the solid curve shows the average cumulative reward over the last 50 training episodes. If less than 50 episodes are trained, the solid curve shows the average of the result over all of the previous trained episodes. The points are grouped into horizontal lines, which correspond to the cumulative reward or battery level when the agent recharges in different catastrophic failure scenarios or when agents successfully complete the training episodes. The result indicates that the MAPPO algorithm successfully trains agents to pursue

Parameter	Parameter Value
$\gamma$	0.95
GAE $\lambda$	1.5e-4
Policy clip	0.15 (T2), 0.14 (T3), 0.13 (T4)
Batch size	128 (T2), 192 (T3), 384 (T4A), 512 (T4B)
Epoch	2 (T4B), 3 (others)
Entropy coefficient	0.02
Learning rate	Start from 2e-3 and decrease 3.75e-6 every 1,250 steps

Table 3: Values of MAPPO hyperparameters.

Parameter	Parameter Value
Penalty for agents running out of battery ( $c_b$ )	50
Reward function $R_i$ 's weight coefficient $w_i$	1
Reward function $R_b$ 's weight $w_b$	2.5

Table 4: Values of reward function parameters.

the maximum cumulative reward and that agents successfully learn an efficient battery recharging strategy as the cumulative reward increases and the battery level at recharge decreases. However, the results also show that the agents recharge with less than 10% battery remaining. This is caused by the use of the linear scalarization method in the multi-objective reward function, i.e., an agent may pursue one objective and sacrifice others, as the summation of the reward components might still be larger. From Fig. 5, we can see that some horizontal lines which correspond to catastrophic failure scenarios persist, which indicates that the catastrophic failure rate barely decreases since the agents are attempting to drain their battery when agents are trained more.

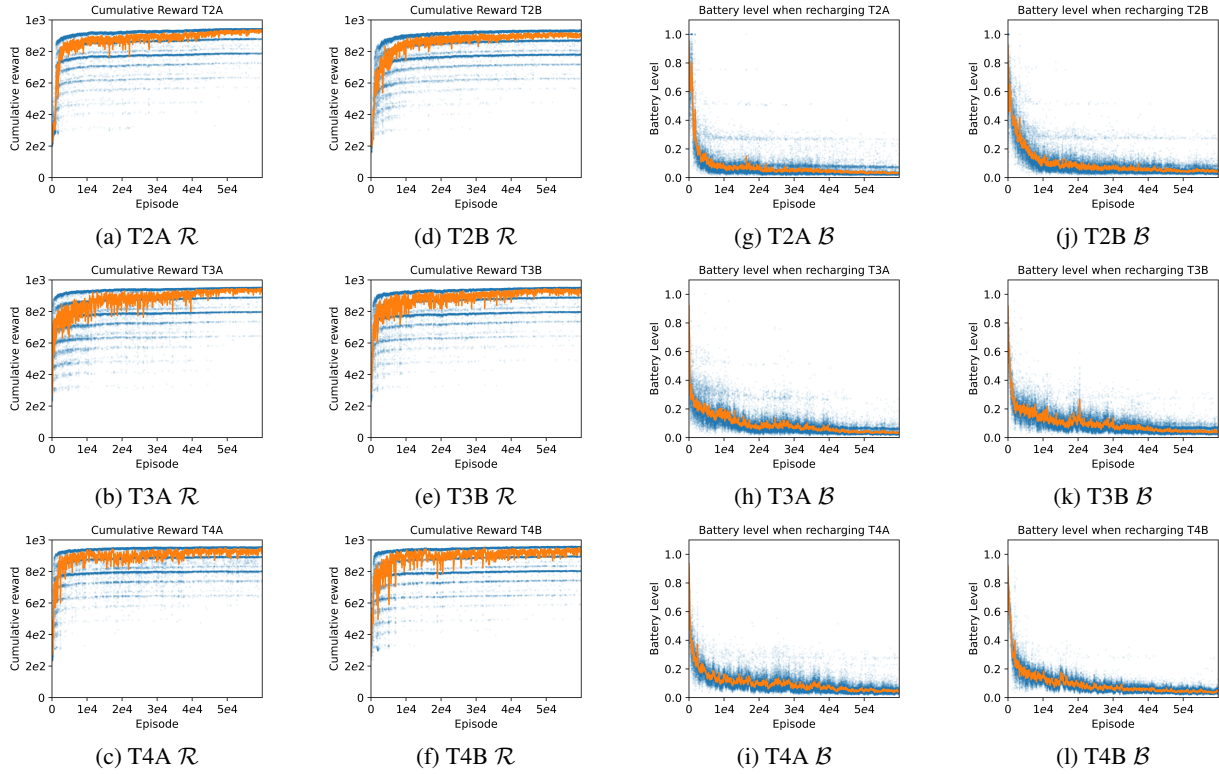


Figure 5: Training results. "R" stands for "cumulative reward". "B" stands for "battery level when recharging". The points are the data of an episode. The solid curve shows the average of the last 50 episodes' data.

## 6.2 Performance Evaluation

The horizon of a test episode is 5,200 steps, where the first 200 steps are considered warm-up steps. Three metrics are used to evaluate a strategy's performance: the value of the criteria  $AVG^h(G_t)$  and  $MAX^h(G)$ , and the average battery level when agents recharge. The performance metrics for a given strategy are estimated based on data collected from 100 successfully completed episodes with no catastrophic failures. If an idleness failure or battery failure occurs, the test episode is terminated, and the failure rate is calculated based on 10 completion rates of 100 test episodes.

### 6.2.1 Battery Recharging Performance Evaluation

In this experiment, the deep MARL-based strategy trained with  $n$  agents is deployed on  $n$  agents to run test episodes. Table. 5 shows the average of the remaining battery level when agents recharge. The result shows that the agents will recharge with less than 10% battery remaining. Table. 7<sup>4</sup> shows the failure rate of agents, where the average of the battery failure rate on Map A is approximately 6%, and on Map B, which has a higher complexity, approximately 16%. Although the agents can successfully recharge most of the time, the failure rate of the patrolling system grows with respect to the number of patrolling agents. This makes it impractical to deploy a patrolling strategy with an overly large number of patrolling agents.

Strategy	Battery Level	
	Map A	Map B
T2	0.0287	0.0419
T3	0.0329	0.0369
T4	0.0402	0.0412

Table 5: The remaining battery level ( $\in [0, 1]$ ) when agents recharge.

To understand the reason for agent battery failures, screenshots (Fig. 6) of the simulation’s graphical interface show several battery failure scenarios on the two maps. The battery-drained agents are shown in black, while the other agents are shown in grey. From the graph, we can see that in many failure cases (e.g. Fig. 6a, Fig. 6c, Fig. 6e, Fig. 6g), the battery-drained agents may be only a few steps away from the battery charging station. This indicates that battery failures may often occur when agents are on the way to the battery charging station. To further assess such a scenario and with the aim of reducing the battery failure rate, we introduce a backup battery to the agents, which allows them to move a few more steps after their main battery is drained. We consider a small backup battery that only allows an agent to move 15 steps. The backup battery is recharged when the agent recharges its main battery at the charging station.

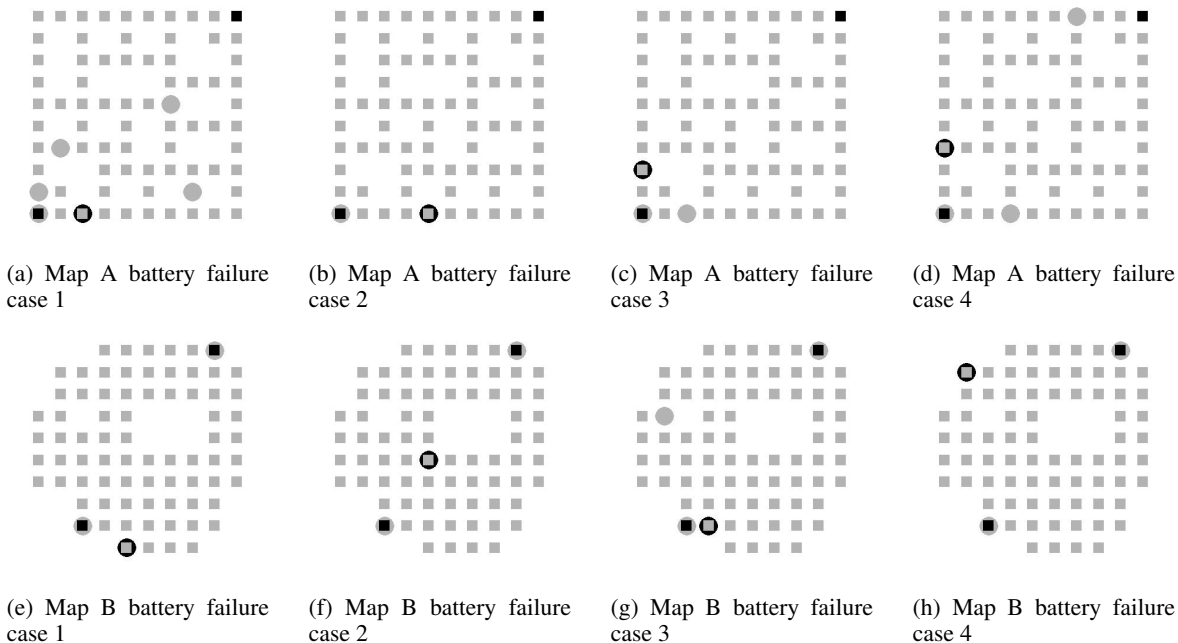


Figure 6: Example battery failure cases. The agents that run out of batteries are painted black.

Table 7 shows the failure rate after the backup battery is introduced. In this case, we see that the battery failure rate of the agents has been successfully reduced. Therefore, we can conclude that the deep MARL-based strategy we developed successfully trained the agents to recharge, and the backup battery can successfully reduce the battery

<sup>4</sup>Overfitting is observed during the training of T4A. The model used for T4A in the following tests is fine-tuned, where the model is trained for another 300 episodes with the entropy coefficient set to 0.08 after 59,000 training episodes

Strategy	Failure Rate					
	Map A		Map B		Map B	
	<b>IF</b>	<b>BF</b>	<b>IF</b>	<b>BF</b>	<b>IF</b>	<b>BF</b>
T2	$\mu = 0, \delta = 0$	$\mu = 0.060, \delta = 0.0267$	$\mu = 0, \delta = 0$	$\mu = 0.124, \delta = 0.0347$	$\mu = 0, \delta = 0$	$\mu = 0.124, \delta = 0.0347$
T3	$\mu = 0, \delta = 0$	$\mu = 0.041, \delta = 0.0185$	$\mu = 0, \delta = 0$	$\mu = 0.156, \delta = 0.0344$	$\mu = 0, \delta = 0$	$\mu = 0.156, \delta = 0.0344$
T4	$\mu = 0, \delta = 0$	$\mu = 0.108, \delta = 0.0297$	$\mu = 0, \delta = 0$	$\mu = 0.206, \delta = 0.0477$	$\mu = 0, \delta = 0$	$\mu = 0.206, \delta = 0.0477$

Table 6: Deep MARL-based strategies' failure rate of agents without a backup battery. **IF** – Idleness failure rate, **BF** – Battery failure rate,  $\mu$  – the average of the failure rate,  $\delta$  – the variance of the failure rate

Strategy	Failure Rate					
	Map A		Map B		Map B	
	IF	BF	IF	BF	IF	BF
T2	$\mu = 0, \delta = 0$	$\mu = 0, \delta = 0$	$\mu = 0, \delta = 0$	$\mu = 0, \delta = 0$	$\mu = 0.008, \delta = 0.0092$	$\mu = 0.008, \delta = 0.0092$
T3	$\mu = 0, \delta = 0$	$\mu = 0.001, \delta = 0.0032$	$\mu = 0, \delta = 0$	$\mu = 0, \delta = 0$	$\mu = 0.001, \delta = 0.0032$	$\mu = 0.001, \delta = 0.0032$
T4	$\mu = 0, \delta = 0$	$\mu = 0.003, \delta = 0.0048$	$\mu = 0, \delta = 0$	$\mu = 0, \delta = 0$	$\mu = 0.005, \delta = 0.0071$	$\mu = 0.005, \delta = 0.0071$

Table 7: Deep MARL-based failure rate of agents with a backup battery.

failure rate. However, we can also conclude that the linear scalarization reward function has a limited effect on training agents to recharge with approximately 10% battery remaining.

In the remainder of the experiments, we assume the backup battery is installed in the agents when running test episodes.

### 6.2.2 Patrolling Performance Evaluation

The patrolling performance of the deep MARL-based strategies is compared to the CC and CR strategies. For simplicity, the following convention is used for the CC and CR strategies:  $CC/CRnA/B$ . For example,  $CC3B$  represents the CC strategy used with 3 agents on Map B. In cases in which the map is not relevant,  $CC/CRnA/B$  is abbreviated as  $CC/CRn$ . The deep MARL-based strategy trained with  $n$  agents will be deployed to  $n$  agents to run test episodes and compared with the corresponding  $CCn$  and  $CRn$  strategies. It is worth noting that deep MARL-based agents do not recharge exactly with 10% battery remaining. Therefore, when comparing the patrolling performance of the strategies, for fairness, CC and CR agents and deep MARL-based agents are set to recharge with approximately the same amount of battery level remaining.

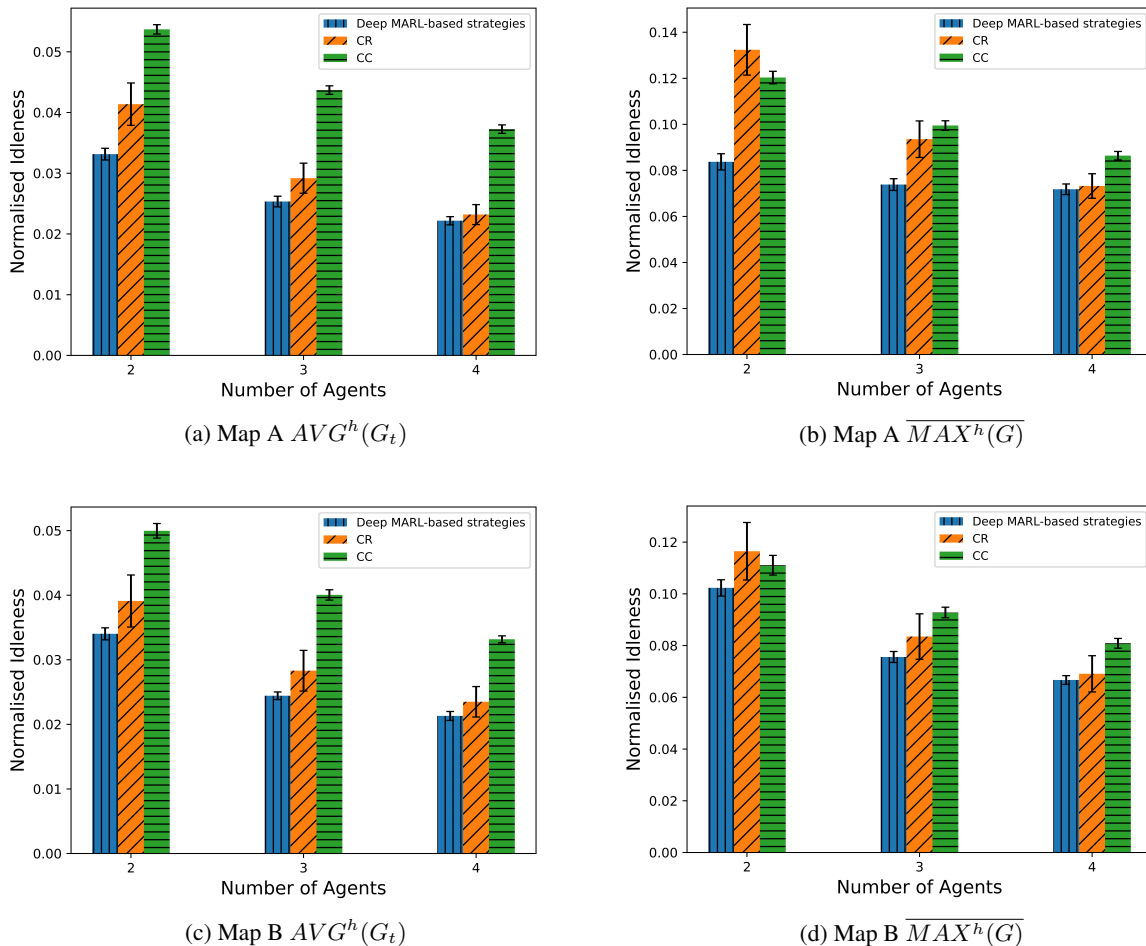


Figure 7: The value of criteria  $AVG^h(G_t)$  and  $\overline{MAX^h(G)}$  of strategies on both maps

Fig. 7 shows the value of  $AVG^h(G_t)$  and  $\overline{MAX^h(G)}$  for the strategies on both maps. Table 7 shows the deep MARL-based strategy failure rate. From the results, we can see that the average performance of deep MARL-based strategies  $T2$  and  $T3$  greatly surpass both CC and CR strategies when evaluated using both criteria, while the average performance of the  $T4$  strategy slightly surpasses the CC and CR strategies. All models have a near 0 idleness failure rate and a low battery failure rate with the backup battery installed. Therefore, we can conclude that the proposed deep

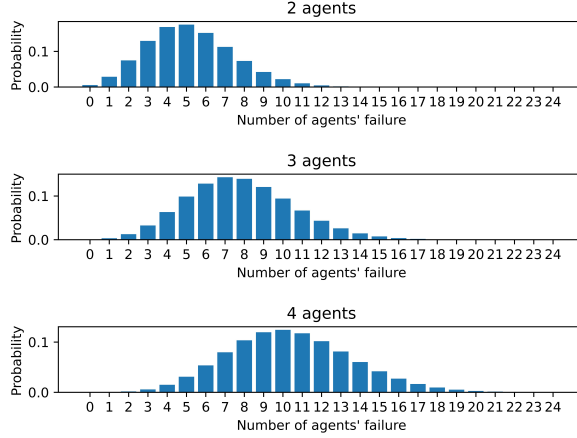


Figure 8: Probability distribution of the number of agent failures that may occur in a test episode with 2, 3, 4 agents

MARL patrolling strategy can effectively patrol the map with battery constraints whilst lowering both the average and maximum idleness times.

### 6.2.3 Robustness Evaluation

In this test, the strategies' patrolling and battery recharging performance are analysed in situations in which agents fail, and supplementary agents are introduced. The evaluation method for the patrolling and battery recharging performance is identical to the method used in Section 6.2.2 and Section 6.2.1.

To simulate agent failure scenarios, it is assumed that the agent has a 0.05% failure rate at every step. When an agent fails, it will be removed from the patrolling map, and a supplementary agent will start to be prepared for deployment from one of the battery charging stations. An agent running out of battery is still considered a catastrophic failure, i.e., battery failed agents will not be replaced by supplementary agents, and the episode will be terminated. Fig. 8 shows the probability distribution of the number of failures in the patrolling system that may occur in a test episode with respect to the number of agents in the system.

Fig. 9 shows the value of  $AVG^h(G_t)$  and  $\overline{MAX^h(G)}$  of the  $T2$ ,  $T3$ , and  $T4$  strategies in scenarios with/without agent failures. Table. 8 shows their failure rate. We see that the performance of the patrolling strategies does not degrade significantly when agent failures occur, and the idleness and battery failure rates are increased. In addition, the variance of the agent's performance may increase in failure scenarios.

If we assume one step in the simulation corresponds to 10 seconds in the real world, the hourly failure rate of a patrolling system with two agents is approximately 0.34, which is much higher than the failure rate of real-world autonomous vehicles such as commercial UAVs [19]. As such, the effect of an agent failure in the real world will be less than the effect in these scenarios.

To simulate scenarios when supplementary agents are introduced, the deep MARL-based strategy trained with  $n$  agents is deployed with  $n + 1$ ,  $n + 2$ , and  $n + 3$  agents to run test episodes. For simplicity, we use the following convention to name the tests:  $TnRmA/B$  represents a model trained with  $n$  agents deployed to  $m$  agents to run the test episodes. In cases in which the map is not relevant,  $TnRmA/B$  is abbreviated as  $TnRm$ . A deep-MARL strategy  $TnRm$  performance is then compared with the  $CCm$  and  $CRm$  strategies.

Fig. 10 shows the value of criteria  $AVG^h(G_t)$  and  $\overline{MAX^h(G)}$  of the strategies in scenarios where supplementary agents are introduced. Table 9 shows the deep MARL-based failure rate. The results show that when supplementary agents are introduced, the deep MARL-based agents can cooperate well with existing agents in the patrolling system, with a slight and unavoidable increase in the failure rate as more agents are added to the system. In addition, the deep MARL-based performance increases when supplementary agents are introduced, and the average performance of deep MARL-based strategies surpasses the CC and CR strategies in all tests, thereby demonstrating the robustness of the deep MARL-based strategy.

However, when comparing the performance of deep-MARL strategies, we can see that the average performance of  $T3Rn$  will sometimes surpass  $T4Rn$  (Fig. 11), i.e., when the number of learning agents increases, it can be harder to

Strategy	Failure Rate					
	Map A		Map B		Map B	
	IF	BF	IF	BF	IF	BF
T2	$\mu = 0.008, \delta = 0.0092$	$\mu = 0, \delta = 0$	$\mu = 0, \delta = 0$	$\mu = 0, \delta = 0$	$\mu = 0.016, \delta = 0.0107$	$\mu = 0.016, \delta = 0.0107$
T3	$\mu = 0.001, \delta = 0.0032$	$\mu = 0, \delta = 0$	$\mu = 0.001, \delta = 0.0032$	$\mu = 0.004, \delta = 0.0070$	$\mu = 0.004, \delta = 0.0070$	$\mu = 0.004, \delta = 0.0070$
T4	$\mu = 0, \delta = 0$	$\mu = 0.031, \delta = 0.01524$	$\mu = 0, \delta = 0$	$\mu = 0, \delta = 0$	$\mu = 0.006, \delta = 0.0070$	$\mu = 0.006, \delta = 0.0070$

Table 8: Deep MARL-based strategies' failure rate in agent failure scenarios.

Strategy	Failure Rate			
	Map A		Map B	
	IF	BF	IF	BF
T2R3	$\mu = 0, \delta = 0$	$\mu = 0, \delta = 0$	$\mu = 0, \delta = 0$	$\mu = 0.007, \delta = 0.0095$
T2R4	$\mu = 0, \delta = 0$	$\mu = 0, \delta = 0$	$\mu = 0, \delta = 0$	$\mu = 0.009, \delta = 0.0070$
T2R5	$\mu = 0, \delta = 0$	$\mu = 0, \delta = 0$	$\mu = 0, \delta = 0$	$\mu = 0.010, \delta = 0.0100$
T3R4	$\mu = 0, \delta = 0$	$\mu = 0.001, \delta = 0.0032$	$\mu = 0, \delta = 0$	$\mu = 0.003, \delta = 0.0048$
T3R5	$\mu = 0, \delta = 0$	$\mu = 0, \delta = 0$	$\mu = 0, \delta = 0$	$\mu = 0, \delta = 0$
T3R6	$\mu = 0, \delta = 0$	$\mu = 0.004, \delta = 0.0070$	$\mu = 0, \delta = 0$	$\mu = 0.007, \delta = 0.0095$
T4R5	$\mu = 0, \delta = 0$	$\mu = 0.005, \delta = 0.0070$	$\mu = 0, \delta = 0$	$\mu = 0.005, \delta = 0.0070$
T4R6	$\mu = 0, \delta = 0$	$\mu = 0.008, \delta = 0.0092$	$\mu = 0, \delta = 0$	$\mu = 0.008, \delta = 0.0092$
T4R7	$\mu = 0, \delta = 0$	$\mu = 0.006, \delta = 0.0084$	$\mu = 0, \delta = 0$	$\mu = 0.019, \delta = 0.0099$

Table 9: Deep MARL-based Strategies' Failure Rate in Scenarios where supplementary agents are introduced.

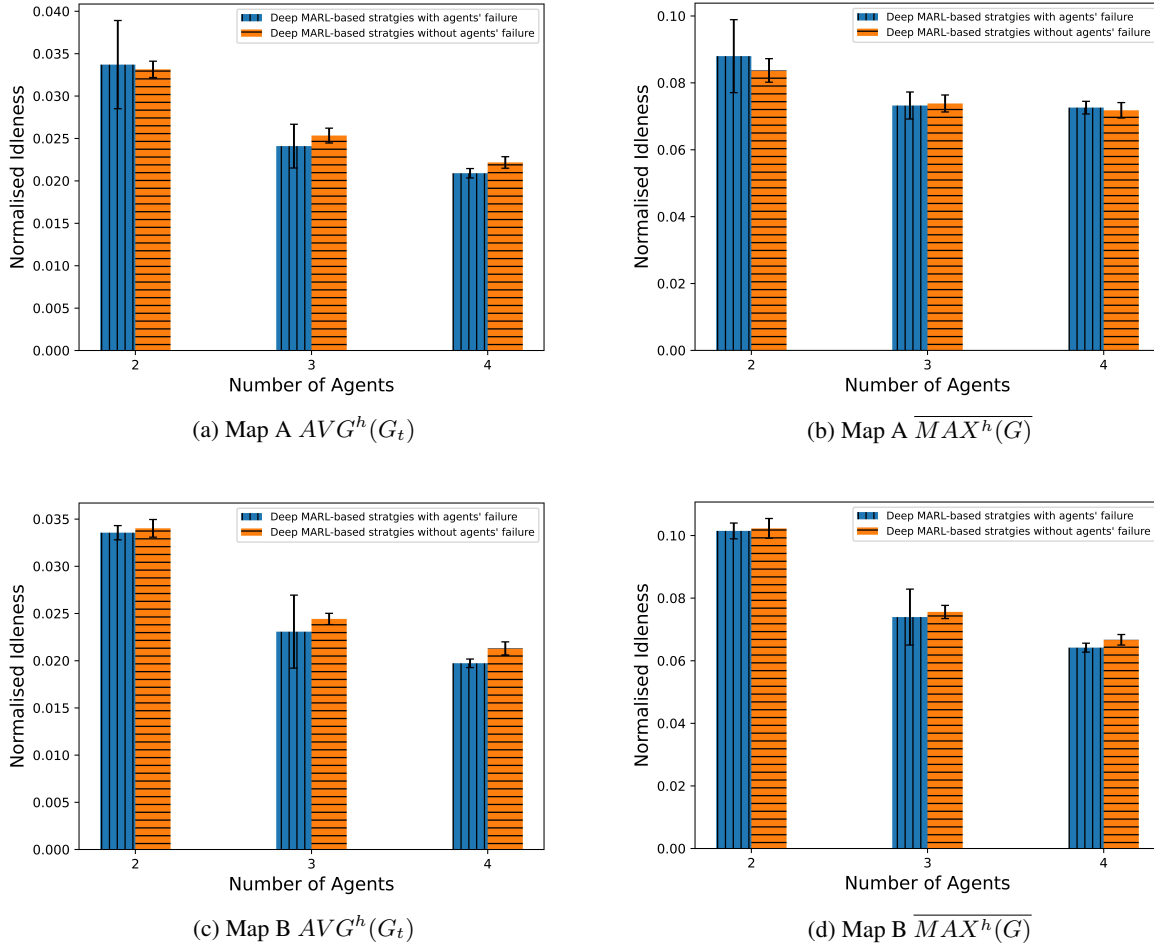


Figure 9: The value of criteria  $AVG^h(G_t)$  and  $\overline{MAX^h(G)}$  of deep-MARL strategies on both maps in scenarios where agents fail versus scenarios without agent failures.

train agents to find the optimal patrolling strategy. One possible reason for this is the well-known instability issues of MARL [3]. Namely, multiple agents are altering their policies at the same time, which results in constant changes in the environment dynamic, thereby preventing the agent's policy from converging. Another illustration of this is shown in Fig. 5a to Fig. 5f where we can see that the variance of the cumulative reward the agent gains during training is larger when there are more patrolling agents in the system. One possible solution to the instability problem is transfer learning. Since a homogeneous architecture is used, the policy trained with fewer agents can be used by other learning agents to continue the training to guarantee a baseline performance. However, multi-agent reinforcement learning transfer is outside the scope of this research.

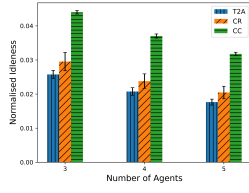
#### 6.2.4 Adaptability to Environment Dynamics

To simulate dynamics in the environment, we assume that at each step, there is a probability  $p$  that the agent will randomly move in a given direction. The value of  $p$  is randomly chosen from  $[0, 1]$  at each step for each agent. If the random action results in the agent hitting an obstacle, the agent will remain at its current location. If the random action results in an agent landing on the battery charging station, the agent will not be recharged.

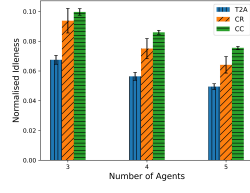
Fig. 12 shows the values of  $AVG^h(G_t)$  and  $\overline{MAX^h(G)}$  of the deep MARL-based strategies in the environment with/without dynamics. Table. 10 shows the deep MARL-based strategies' failure rate. The result shows that even without training the deep-MARL strategies specifically adapt to deal with environment dynamics. In this case, the

Strategy	Failure Rate					
	Map A		Map B		Map B	
	IF	BF	IF	BF	IF	BF
T2	$\mu = 0.001, \delta = 0.0032$	$\mu = 0, \delta = 0$	$\mu = 0, \delta = 0$	$\mu = 0, \delta = 0$	$\mu = 0.037, \delta = 0.0125$	$\mu = 0.037, \delta = 0.0125$
T3	$\mu = 0, \delta = 0$	$\mu = 0.002, \delta = 0.0042$	$\mu = 0, \delta = 0$	$\mu = 0, \delta = 0$	$\mu = 0.001, \delta = 0.0032$	$\mu = 0.001, \delta = 0.0032$
T4	$\mu = 0, \delta = 0$	$\mu = 0.003, \delta = 0.0048$	$\mu = 0, \delta = 0$	$\mu = 0, \delta = 0$	$\mu = 0.027, \delta = 0.0116$	$\mu = 0.027, \delta = 0.0116$

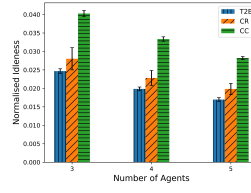
Table 10: Deep MARL-based Failure Rate of Agents in the dynamic environment.



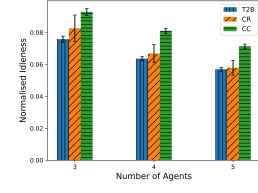
(a) T2A and CC and CR  $AVG^h(G_t)$



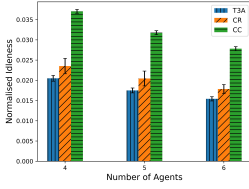
(b) T2A and CC and CR  $\overline{MAX^h(G)}$



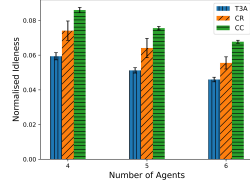
(c) T2B and CC and CR  $AVG^h(G_t)$



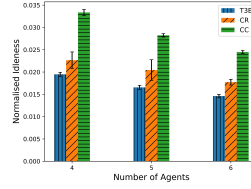
(d) T2B and CC and CR  $\overline{MAX^h(G)}$



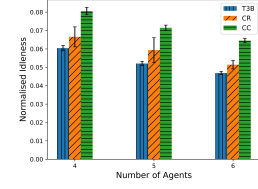
(e) T3A and CC and CR  $AVG^h(G_t)$



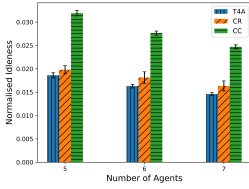
(f) T3A and CC and CR  $\overline{MAX^h(G)}$



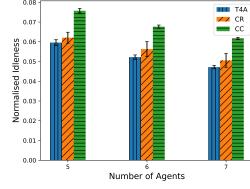
(g) T3B and CC and CR  $AVG^h(G_t)$



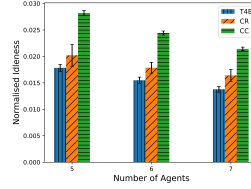
(h) T3B and CC and CR  $\overline{MAX^h(G)}$



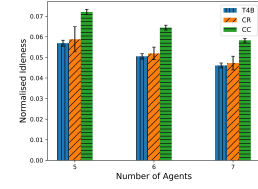
(i) T4A and CC and CR  $AVG^h(G_t)$



(j) T4A and CC and CR  $\overline{MAX^h(G)}$



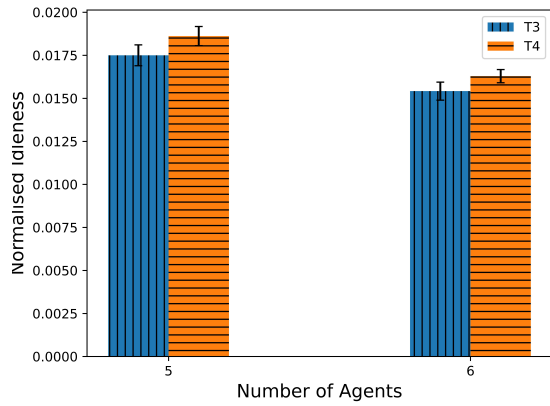
(k) T4B and CC and CR  $AVG^h(G_t)$



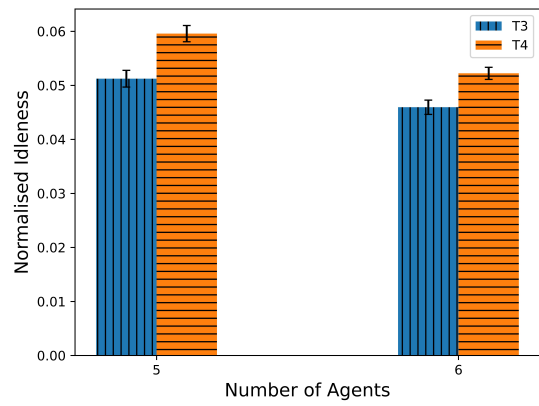
(l) T4B and CC and CR  $\overline{MAX^h(G)}$

Figure 10: The value of criteria  $AVG^h(G_t)$  and  $\overline{MAX^h(G)}$  of the strategies in scenarios where supplementary agents are introduced

performance of the patrolling strategies is not reduced significantly and the failure rate does not increase significantly. Therefore, agent adaptability to deal with dynamic environments is supported.

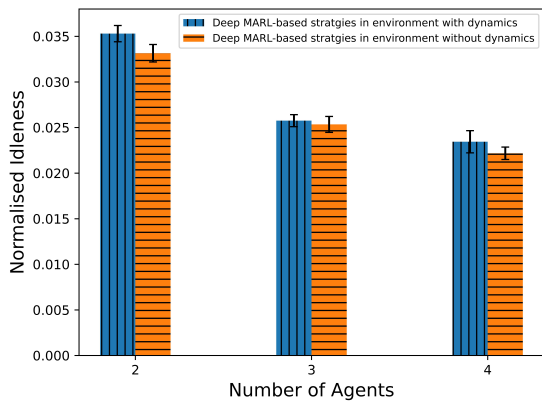


(a) Map A  $AVG^h(G_t)$

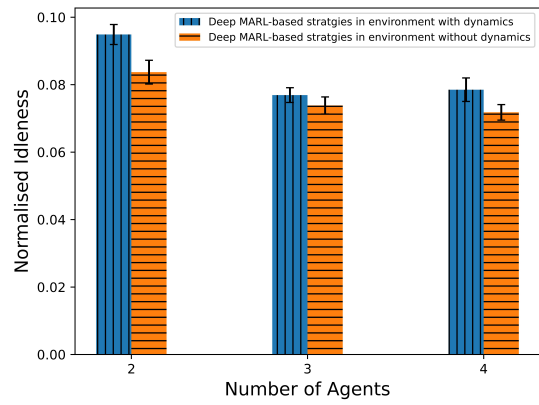


(b) Map A  $\overline{MAX^h(G)}$

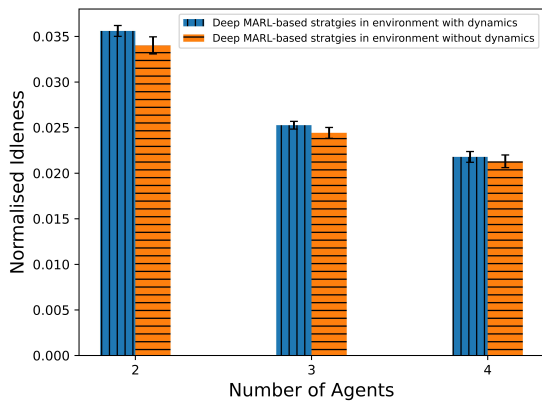
Figure 11: The value of criteria  $AVG^h(G_t)$  and  $\overline{MAX^h(G)}$  of T3R5, T3R6 vs T4R5 and T4R6 on Map A



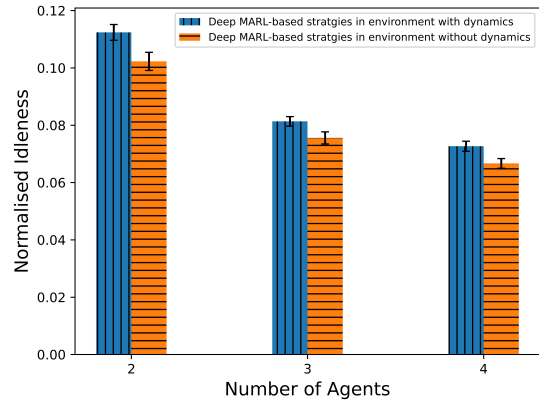
(a) Map A  $AVG^h(G_t)$



(b) Map A  $\overline{MAX^h(G)}$



(c) Map B  $AVG^h(G_t)$



(d) Map B  $\overline{MAX^h(G)}$

Figure 12: The value of criteria  $AVG^h(G_t)$  and  $\overline{MAX^h(G)}$  of deep-MARL strategies on both maps in the environment with dynamics versus in the environment without dynamics

## 7 Conclusion

This work has proposed a deep reinforcement learning based approach for multi-agent patrolling problems that encompasses multiple constraints impacting real-world autonomous patrolling vehicles. A homogeneous multi-agent architecture is proposed where agents execute identical policies. This supports a robust patrolling system that can tolerate agent failures and allow supplementary agents to be added to either replace failed agents or increase the patrolling performance. We use a state-of-the-art reinforcement learning algorithm (Proximal Policy Optimization) to train the patrolling agents with different numbers of agents. The simulation experiments show that our approach can successfully reduce both the average and maximum idleness incurred during patrolling factoring in battery constraints. The performance surpasses the CC and CR strategies. In addition, the robustness of the approach and its adaptability to environment dynamics has been demonstrated.

There are several areas that could be explored in future extensions to the work, including:

- addressing the instability in training that increases when the number of learning agents increases;
- assumptions of ideal communication channels where the communication between agents has no cost, delay or failures. This is unlikely to be the case in the real world. Such uncertainties in communication need to be taken into account.
- dealing with the distributed state of agents, e.g. where shared information is needed to optimise the patrolling. This might for example be where one agent identifies an intruder and the other agents navigate to that area of the grid to track/capture the intruder.
- deploying the solution to real-world patrolling vehicles.

## **8 Acknowledgement**

This research was supported by use of the Nectar Research Cloud, a collaborative Australian research platform supported by the NCRIS-funded Australian Research Data Commons (ARDC)

This study was supported by the *Melbourne Research Scholarship* from the Univerisity of Melbourne, VIC, Australia.

## References

- [1] Alessandro Almeida, Geber Ramalho, Hugo Santana, Patricia Tedesco, Talita Menezes, Vincent Corruble, and Yann Chevalyere. Recent advances on multi-agent patrolling. pages 474–483, 09 2004.
- [2] Nicola Basilico. Recent trends in robotic patrolling. *Current Robotics Reports*, 3, 06 2022.
- [3] Lorenzo Canese, Gian Carlo Cardarilli, Luca Di Nunzio, Rocco Fazzolari, Daniele Giardino, Marco Re, and Sergio Span. Multi-agent reinforcement learning: A review of challenges and applications. *Applied Sciences*, 11(11), 2021.
- [4] Y. Chevalyere. Theoretical analysis of the multi-agent patrolling problem. In *Proceedings. IEEE/WIC/ACM International Conference on Intelligent Agent Technology, 2004. (IAT 2004).*, pages 302–308, 2004.
- [5] Carolina Rutili De Lima, Said Ghani Khan, Syed Humayoon Shah, and Cheng-Kai Lu. Deliberative/reactive architecture of a multirobot patrol system based on supervisory control theory. *IEEE Sensors Journal*, 22(11):11023–11033, 2022.
- [6] Alessandro de Luna Almeida, Pedro Machado de Castro, Talita Menezes, and Geber Ramalho. Combining idleness and distance to design heuristic agents for the patrolling task. 2003.
- [7] Yotam Elor and Alfred M. Bruckstein. Autonomous multi-agent cycle based patrolling. In Marco Dorigo, Mauro Birattari, Gianni A. Di Caro, René Doursat, Andries P. Engelbrecht, Dario Floreano, Luca Maria Gambardella, Roderich Groß, Erol Şahin, Hiroki Sayama, and Thomas Stützle, editors, *Swarm Intelligence*, pages 119–130, Berlin, Heidelberg, 2010. Springer Berlin Heidelberg.
- [8] Milan Erdelj, Micha Krl, and Enrico Natalizio. Wireless sensor networks and multi-uav systems for natural disaster management. *Computer Networks*, 124:72–86, 2017.
- [9] Milan Erdelj, Enrico Natalizio, Kaushik R. Chowdhury, and Ian F. Akyildiz. Help from the sky: Leveraging uavs for disaster management. *IEEE Pervasive Computing*, 16(1):24–32, 2017.
- [10] Hailong Huang, Andrey V. Savkin, and Chao Huang. Decentralized autonomous navigation of a uav network for road traffic monitoring. *IEEE Transactions on Aerospace and Electronic Systems*, 57(4):2558–2564, 2021.
- [11] Meghdeep Jana, Leena Vachhani, and Arpita Sinha. A deep reinforcement learning approach for multi-agent mobile robot patrolling. *International Journal of Intelligent Robotics and Applications*, 2022.
- [12] Elizabeth Jensen, Michael Franklin, Sara Lahr, and Maria Gini. Sustainable multi-robot patrol of an open polyline. In *2011 IEEE International Conference on Robotics and Automation*, pages 4792–4797, 2011.
- [13] Fabrice Lauri and Abderrafiaa Koukam. Robust multi-agent patrolling strategies using reinforcement learning. In *International Conference on Swarm Intelligence Based Optimization*, pages 157–165. Springer, 2014.
- [14] Ryan Lowe, Yi I Wu, Aviv Tamar, Jean Harb, OpenAI Pieter Abbeel, and Igor Mordatch. Multi-agent actor-critic for mixed cooperative-competitive environments. *Advances in neural information processing systems*, 30, 2017.
- [15] Samuel Yanes Luis, Daniel Gutierrez Reina, and Sergio L. Toral Marn. A multiagent deep reinforcement learning approach for path planning in autonomous surface vehicles: The ypacara lake patrolling case. *IEEE Access*, 9:17084–17099, 2021.
- [16] Aydano Machado, Geber Ramalho, Jean-Daniel Zucker, and Alexis Drogoul. Multi-agent patrolling: An empirical analysis of alternative architectures. In *Proceedings of the 3rd International Conference on Multi-Agent-Based Simulation II, MABS’02*, page 155170, Berlin, Heidelberg, 2002. Springer-Verlag.
- [17] Tao Mao and Laura Ray. Frequency-based patrolling with heterogeneous agents and limited communication, 2014.
- [18] Alessandro Marino and Gianluca Antonelli. Experiments on sampling/patrolling with two autonomous underwater vehicles. *Robotics and Autonomous Systems*, 67:61–71, 2015. Advances in Autonomous Underwater Robotics.
- [19] Enrico Petritoli, Fabio Leccese, and Lorenzo Ciani. Reliability and maintenance analysis of unmanned aerial vehicles. *Sensors*, 18(9):3171, 2018.
- [20] David Portugal and Rui P Rocha. Distributed multi-robot patrol: A scalable and fault-tolerant framework. *Robotics and Autonomous Systems*, 61(12):1572–1587, 2013.
- [21] David Portugal and Rui P Rocha. Scalable, fault-tolerant and distributed multi-robot patrol in real world environments. In *2013 IEEE/RSJ International Conference on Intelligent Robots and Systems*, pages 4759–4764. IEEE, 2013.

- [22] David Portugal and Rui P Rocha. Cooperative multi-robot patrol with bayesian learning. *Autonomous Robots*, 40(5):929–953, 2016.
- [23] Tiago Sak, Jacques Wainer, and Siome Goldenstein. Probabilistic multiagent patrolling. pages 124–133, 10 2008.
- [24] H. Santana, G. Ramalho, V. Corruble, and B. Ratitch. Multi-agent patrolling with reinforcement learning. In *Proceedings of the Third International Joint Conference on Autonomous Agents and Multiagent Systems, 2004. AAMAS 2004.*, pages 1122–1129, 2004.
- [25] John Schulman, Sergey Levine, Pieter Abbeel, Michael Jordan, and Philipp Moritz. Trust region policy optimization. In *International conference on machine learning*, pages 1889–1897. PMLR, 2015.
- [26] John Schulman, Filip Wolski, Prafulla Dhariwal, Alec Radford, and Oleg Klimov. Proximal policy optimization algorithms, 2017.
- [27] Aydın Sipahioglu, Gokhan Kirlik, Osman Parlaktuna, and Ahmet Yazici. Energy constrained multi-robot sensor-based coverage path planning using capacitated arc routing approach. *Robotics and Autonomous Systems*, 58(5):529–538, 2010.
- [28] R. Stranders, E. Munoz de Cote, A. Rogers, and N.R. Jennings. Near-optimal continuous patrolling with teams of mobile information gathering agents. *Artificial Intelligence*, 195:63–105, 2013.
- [29] Ayumi Sugiyama, Lingying Wu, and Toshiharu Sugawara. Learning of activity cycle length based on battery limitation in multi-agent continuous cooperative patrol problems. pages 62–71, 01 2019.
- [30] Ashleigh Townsend, Immanuel N. Jiya, Christiaan Martinson, Dmitri Bessarabov, and Rupert Gouws. A comprehensive review of energy sources for unmanned aerial vehicles, their shortfalls and opportunities for improvements. *Heliyon*, 6(11):e05285, 2020.
- [31] Carlos A. Trasvia-Moreno, Rubn Blasco, Ivaro Marco, Roberto Casas, and Armando Trasvia-Castro. Unmanned aerial vehicle based wireless sensor network for marine-coastal environment monitoring. *Sensors*, 17(3), 2017.
- [32] Oriol Vinyals, Igor Babuschkin, Wojciech M. Czarnecki, Michal Mathieu, Andrew Dudzik, Junyoung Chung, David H. Choi, Richard Powell, Timo Ewalds, Petko Georgiev, Junhyuk Oh, Dan Horgan, Manuel Kroiss, Ivo Danihelka, Aja Huang, Laurent Sifre, Trevor Cai, John P. Agapiou, Max Jaderberg, Alexander S. Vezhnevets, Rémi Leblond, Tobias Pohlen, Valentin Dalibard, David Budden, Yury Sulsky, James Molloy, Tom L. Paine, Caglar Gulcehre, Ziyu Wang, Tobias Pfaff, Yuhuai Wu, Roman Ring, Dani Yogatama, Dario Wünsch, Katrina McKinney, Oliver Smith, Tom Schaul, Timothy Lillicrap, Koray Kavukcuoglu, Demis Hassabis, Chris Apps, and David Silver. Grandmaster level in StarCraft II using multi-agent reinforcement learning. *Nature*, 575(7782):350–354, October 2019.
- [33] Bernt Wiandt and Vilmos Simon. Autonomous graph partitioning for multi-agent patrolling problems. pages 261–268, 09 2018.
- [34] Ronald J Williams. Simple statistical gradient-following algorithms for connectionist reinforcement learning. *Machine learning*, 8(3):229–256, 1992.
- [35] Jianhua Yang, Zhaowei Ding, and Lei Wang. The programming model of air-ground cooperative patrol between multi-uav and police car. *IEEE Access*, 9:134503–134517, 2021.
- [36] Chao Yu, Akash Velu, Eugene Vinitzky, Yu Wang, Alexandre Bayen, and Yi Wu. The surprising effectiveness of ppo in cooperative, multi-agent games, 2021.
- [37] Xin Zhou, Weiping Wang, Tao Wang, Yonglin Lei, and Fangcheng Zhong. Bayesian reinforcement learning for multi-robot decentralized patrolling in uncertain environments. *IEEE Transactions on Vehicular Technology*, 68(12):11691–11703, 2019.